analytical chemistry

Article

pubs.acs.org/ac

Wafer-Scale Fabrication of Nanofluidic Arrays and Networks Using Nanoimprint Lithography and Lithographically Patterned Nanowire Electrodeposition Gold Nanowire Masters

Aaron R. Halpern, Keith C. Donavan, Reginald M. Penner,* and Robert M. Corn*

Department of Chemistry, University of California-Irvine, Irvine, California 92697, United States

ABSTRACT: Wafer scale (cm^2) arrays and networks of nanochannels were created in polydimethylsiloxane (PDMS) from a surface pattern of electrodeposited gold nanowires in a master-replica process and characterized with scanning electron microscopy (SEM), atomic force microscopy (AFM), and fluorescence imaging measurements. Patterns of gold nanowires with cross-sectional dimensions as small as 50 nm in height and 100 nm in width were prepared on silica substrates using the process of lithographically patterned nanowire electrodeposition (LPNE). These nanowire patterns were then employed as masters for the fabrication of inverse replica nanochannels in a special formulation of PDMS. SEM and AFM measurements verified a linear correlation between the widths and heights of the nanowires and nanochannels over a range of 50 to 500 nm. The PDMS replica was then oxygen plasma-bonded to a glass substrate in order to create a linear array of nanofluidic channels (up to 1 mm in length) filled with solutions of either fluorescent dye or 20 nm diameter fluorescent polymer nanoparticles. Nanochannel continuity and a 99% fill success rate was determined from the fluorescence imaging measurements, and the electrophoretic injection of both dye and nanoparticles in the nanochannel arrays was also demonstrated. Employing a double LPNE fabrication method, this master-replica process was also used to create a large two-dimensional network of crossed nanofluidic channels.

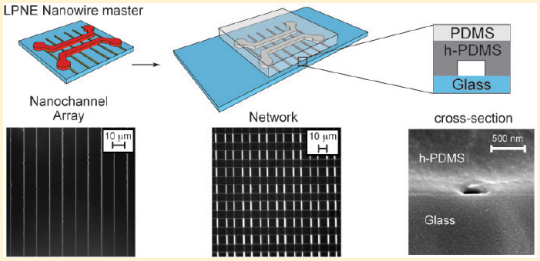

Large area (cm^2) arrays and networks of nanochannels with cross sectional areas of 100 nm × 100 nm or less exhibit unique electrophoretic and fluidic characteristics that have led to their implementation in many applications including separations,[1−3] preconcentration,[4,5] in situ reagent generation,[6] ionic diodes,[7] and the study of the sequence dependent[8−11] transport and internal conformational dynamics[12,13] of DNA. One approach to fabricating nanofluidics is to use brittle materials such as silica or quartz in combination with direct write techniques such as electron beam lithography (EBL)[2,3,11,12,14] or focused ion beam lithography (FIB).[8,15,16] These instruments offer the pinnacle of resolution but suffer in throughput especially for large area applications. In contrast, a second approach in fabricating nanofluidics is the use of soft polymers such as polydimethylsiloxane (PDMS).[17] PDMS is best known for its use in microfluidics that are cheap, easy, and fast to produce through the replication process of soft lithography.[18] Although PDMS is best suited for micrometer sized features, it has been applied to fabricating nanochannels using EBL[19,20] or FIB[21,22] generated masters. However, due to its elasticity, it has difficulty replicating nanostructures below ~200 nm.[23] To overcome this, a number of clever methods for fabricating nanochannels have utilized the unique properties of PDMS, such as wrinkling,[5] fracturing,[24,25] and elastomeric collapse.[26] However, these techniques are often limited in the ability to control position, form complex shapes, and create connectivity for nanochannel networks.

One process that combines the advantages of high resolution from direct write instruments (e.g., EBL or FIB), as well as the high throughput similar to soft lithography, is nanoimprint lithography.[27,28] In this process, a nanoscale master mold generated by EBL (or a variety of other techniques) can be replicated numerous times in a softer thermoplastic or UV curable material by physical contact. The transferred pattern can then be etched into the underlying substrate with resulting feature sizes below 10 nm. NIL has an enormous variety of applications[29,30] including electronics, data storage, and optics, as well as being used to create single nanochannels using an edge patterned master[31] or arrays of nanochannels using interference lithography masters followed by angle deposition[32] or laser melting.[33]

In this paper, we describe an adapted NIL procedure that provides a simple, rapid, wafer-scale method for creating nanofluidic channel networks in PDMS using gold nanowire-on-glass masters fabricated by lithographically patterned nanowire electrodeposition (LPNE)[34−36] in a master-replica process.

EXPERIMENTAL SECTION

Nanowire Master Fabrication. Au nanowire arrays were fabricated on Nochromix cleaned glass slides, with interwire

Received: March 14, 2012
Accepted: April 25, 2012
Published: April 25, 2012

   dx.doi.org/10.1021/ac3007285 | *Anal. Chem.* 2012, 84, 5053−5058

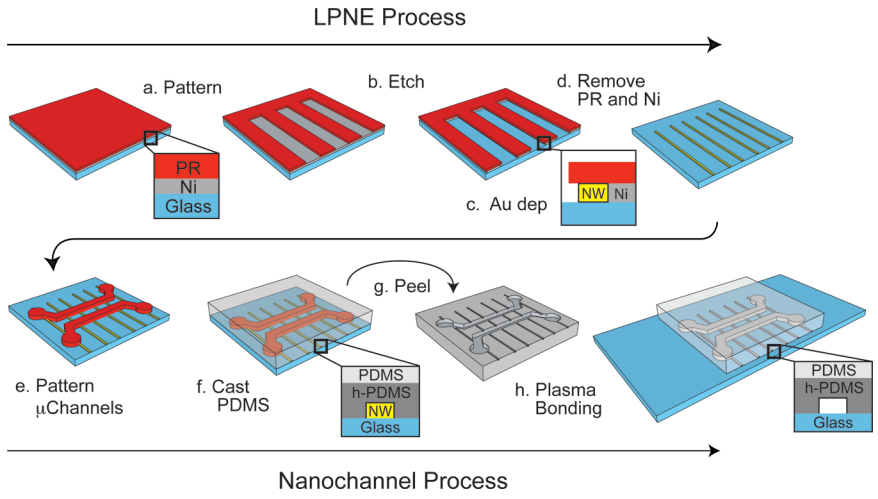

Figure 1. LPNE schematic diagram. (a–d) Gold nanowires are patterned onto a glass substrate using the LPNE process as described in the text. (e) A positive photoresist is patterned on top of the existing nanowire array to create microchannel access to the nanochannels after replication. (f) A thick PDMS layer is cast on top of a spin coated 10 μm underlayer of h-PDMS. (g) The h-PDMS/PDMS is peeled off of the template creating an inverse replica. (h) The replica is bonded to a glass substrate to seal the nanochannel array.

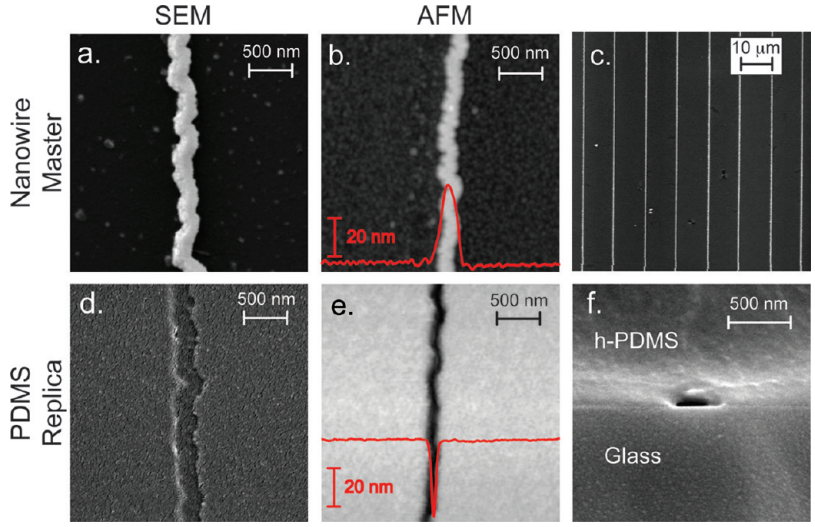

Figure 2. Au master and PDMS replica characterization. (a, b) SEM and AFM image of a single nanowire with width 244 ± 30 nm and height = 47 ± 5 nm, respectively. (c) An 80 μm^2 AFM image showing eight parallel nanowires with 10 μm spacing. (d, e) SEM and AFM image of the PDMS replica with width = 223 ± 28 nm and height = 43 ± 2 nm, respectively. (f) Cross-sectional SEM image of a nanochannel sealed to the glass substrate.

spacing of 10 μm using the LPNE process.[34−36] Shipley 1827 photoresist was obtained from Microchem (Newton, MA) and used to form the microchannel access.

PDMS and Hard PDMS. Sylgard 184 from Dow Corning (Midland, MI) was used in a 10:1 prepolymer to curing agent ratio. All components for the hard PDMS (h-PDMS) were purchased from Gelest (Morrisville, PA) and used as received: A combination of 1.7 g of vinylmethlysiloxane copolymer (VDT-731), 0.05 g of modulator (SIT7900.0), and 9 μL of platinum catalyst (SIP6831.2) were well mixed, followed by addition of 0.5 g of methylhydrosiloxane copolymer (HMS-301).[23] Cured PDMS nanochannel arrays were sealed to cleaned glass slides by exposing both surfaces to a 100 mTorr O_2 plasma for 20 s and then gently placed together and baked at 60 °C for 3 min.

Scanning Electron Microscopy and Atomic Force Microscopy Measurements. Scanning electron microscopy (SEM) images were taken on a Philips XL-30 (North Billerica, MA) at 10 kV. A thin layer of Au/Pd was sputtered onto the samples (1−2 nm for nanowires, 4−5 nm for PDMS) to prevent charging. Atomic force microscopy (AFM) images where acquired on an Asylum Research MFP-3D (Santa Barbara, CA).

Fluorescence Measurements. All nanochannels were imaged with 30 μM Alexa Fluor 488 (Invitrogen, Grand Island, NY) in 0.5× TBE buffer. Low magnification images (4−20×) were acquired on an inverted microscope with a QICAM CCD camera (Qimaging, Surrey, Canada) or an Andor Neo scientific CMOS (South Windsor, CT). High magnification images (40−60× oil immersion) were acquired on an upright microscope with a Princeton CCD camera (Trenton, NJ) or an Andor iXon EMCCD for nanoparticle imaging (20 nm Fluorosphere, Invitrogen).

Electrophoresis. An Autolab PGSTAT12 (Riverview, FL) was used to control the voltage for electrophoresis experiments. All solutions were in 0.5× TBE buffer.

dx.doi.org/10.1021/ac3007285 | *Anal. Chem.* 2012, 84, 5053−5058

RESULTS AND DISCUSSION

Fabrication of Nanowire and Nanochannel Arrays. Our method for fabricating nanochannel arrays is shown schematically in Figure 1. First, a LPNE nanowire master is created as shown in steps a–d: (a) a sacrificial Ni electrode layer is coated with photoresist on top of a glass substrate, and the photoresist is patterned on the micrometer scale by UV lithography; (b) the underlying Ni layer is chemically etched to create a nanoscale undercut "trench"; (c) a gold nanowire is electrodeposited onto the band electrode created in the trench; (d) the photoresist and remaining Ni layer are removed, leaving the gold nanowire array.

This nanowire master is then used to create a nanochannel array as shown schematically in steps e–h of Figure 1: (e) a positive photoresist is patterned on top of the LPNE array to created the micrometer-scale access channels; (f) approximately 10 μm of a formulation of hard PDMS (h-PDMS) is spin-coated onto the entire surface and briefly cured in the oven before a second thick layer of PDMS (~3 mm) is applied to the nanowire master; (g and h) once fully cured, the h-PDMS/PDMS layer is peeled away from the nanowire master and then bonded to a glass substrate using standard O_2 plasma attachment procedures[18] to create the nanochannel arrays. The base layer of h-PDMS is critical for the faithful replication of submicrometer features, as the higher compression modulus of h-PDMS allows the replica to conform and hold the shape of the nanowire master.[23,37] Once the process is complete, the nanowire master can be used again for the reproduction of additional PDMS nanochannel networks. LPNE master molds were replicated six times in succession and showed no sign of degradation; we estimate that they will retain their integrity for up to 50 replication cycles or more.

SEM and AFM Characterization. A set of SEM and AFM measurements were used to characterize the width and height of the nanowire masters and nanochannel replicas. Figure 2 shows both a wide field AFM image of a LPNE nanowire array with parallel wire spacing of 10 μm (Figure 2c) and higher resolution SEM and AFM images of a single Au nanowire from the array with a measured width $w = 244 \pm 30$ nm and a height $h = 47 \pm 5$ nm (Figure 2a,b, respectively).

A second set of SEM and AFM measurements were used to characterize the nanochannels created in the h-PDMS from the LPNE master; typical SEM and AFM images are shown in Figure 2d,e. From theses images, we observe that the measured nanochannel dimensions are very close to those of the master nanowire pattern (Figure 2a,b): $w = 223 \pm 28$ nm and $h = 43 \pm 2$ nm. SEM/AFM measurements were conducted on a series of masters and replicas over a range of widths and heights, and the results are compiled and plotted in Figure 3a,b. We find a 1:1 correspondence of the width and height of the nanochannels reproduced in h-PDMS with the electrodeposited LPNE nanowires over a range of 100 to 500 nm and 45 to 230 nm, respectively. The width and height of the nanochannels can be controlled independently in the LPNE process.

In the final step of the fabrication process, the PDMS replica is attached to a glass substrate to form the nanochannnel array. Figure 2f shows a cross sectional SEM image of a nanochannel created by this bonding process demonstrating retention of the rectangular nature of the master after attachment to a glass surface.

Fluorescence Characterization. As shown schematically in Figure 1h, the nanochannel arrays were fabricated between

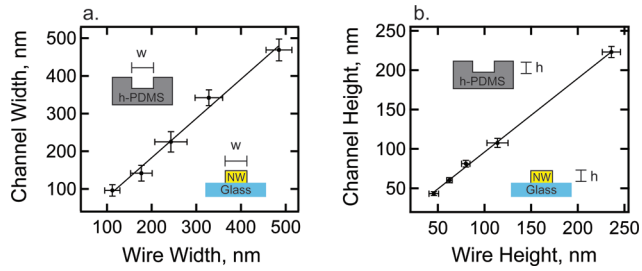

Figure 3. Master-replica calibration. (a) Calibration of nanochannel width versus nanowire width as measured by SEM. Measured widths range from 100 to 500 nm. (b) Calibration for nanochannel height versus nanowire height as measured by AFM. Measured heights range from 43 to 236 nm.

two PDMS microchannels (250 μm width × 3 μm height). Introduction of solutions into the microchannels provided fluidic access to the nanochannels; they filled spontaneously by capillary action from the top and bottom microfluidic channels. Figure 4 shows a series of fluorescence images obtained after

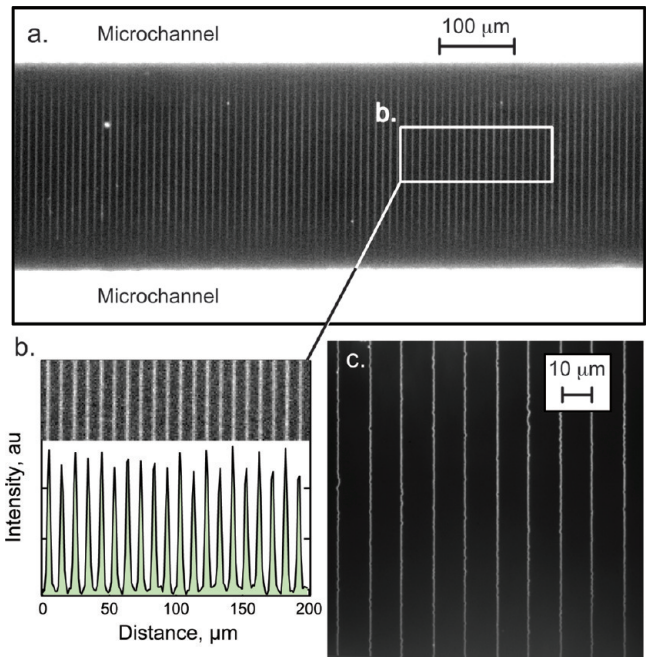

Figure 4. Fluorescence characterization of nanochannels. (a) 4× fluorescence image of 85 vertically aligned nanochannels, 300 μm in length, filled with fluorescent dye between horizontal microchannels. (b) ROI of (a) featuring 20 nanochannels and corresponding fluorescent intensity profile. (c) 60× high magnification image of 10 nanochannels filled with fluorescent dye.

introducing a fluorescent solution into an array of nanochannels with dimensions of 160 nm in width, 70 nm in height, and 300 μm in length. Figure 4a is a 4× magnification image of 85 vertically aligned nanochannels; the bright areas above and below the nanochannel array are the fluorescence from two much larger horizontal microchannels.

Very few defects are observed in these replicated nanochannels; the array in Figure 4 consisted in total of 480 nanochannels, of which only 4 did not fill (99% fidelity). We attribute the small number of faulty nanochannels to imperfections in the LPNE nanowire master. Figure 4b is an expanded region of the 4× fluorescence image from Figure 4a

dx.doi.org/10.1021/ac3007285 | Anal. Chem. 2012, 84, 5053–5058

showing the fluorescence intensity profile of 20 nanochannels. While the width of the fluorescence lines in the image are limited by the optical resolution of the microscope, the integrated intensity is a measure of the concentration of fluorophores in the nanochannel. These quantitative fluorescence measurements confirmed that the channel cross section is very uniform both along the nanochannel and across the entire array. Figure 4c is a 60× magnification image of the fluorescent nanochannels that confirm this uniformity and also shows that the nanochannels replicate all of the fine structure observed in the LPNE nanowire masters. Although we have limited this work to straight channels, it is possible to fabricate more intricate nanochannel geometries such as zig-zags and switch backs using a more complex mask in the LPNE fabrication step.[34]

Electrophoresis of Dye and Nanoparticles. To evaluate the ionic conductivity of the nanochannel arrays for potential electrophoretic separations, a DC voltage was applied across the upper and lower microfluidic channels and the transit of fluorescent species through the nanochannels was monitored in real time. Figure 5a shows a time series of images as a

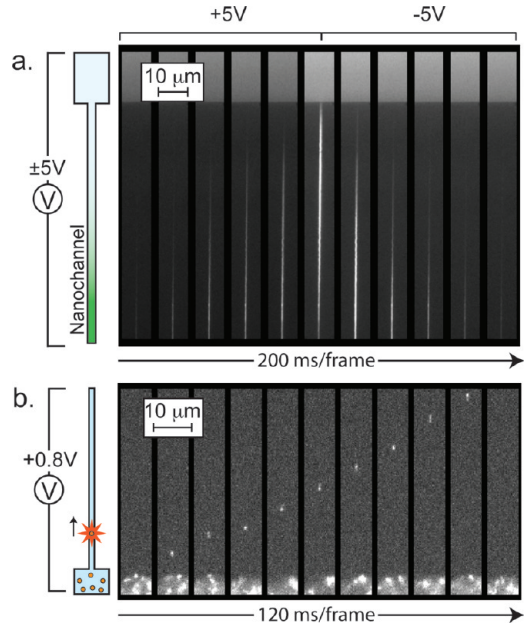

Figure 5. Nanochannel electrophoresis. (a) Electrophoretic flow and reversal of fluorescent dye in a single nanochannel with an applied ±5 V. Frames were acquired every 200 ms. (b) Electrophoretic motion of a 20 nm fluorescent particle flowing though a single channel under an applied +0.8 V. Frames were acquired at 120 ms intervals with 30 ms integration time.

fluorescent solution was driven from the bottom microfluidic channel into the nanochannel array (only a single nanochannel is shown in the images). The dimensions of the nanochannels in this experiment are 210 nm width × 75 nm height × 200 μm length. An applied voltage of +5 V across the array resulted in a current of ∼5 pA/nanochannel. When the voltage was flipped to −5 V, the direction of the dye molecules was reversed. It took approximately 2.5 s to completely fill and discharge the nanochannel; no residual fluorescence due to dye adsorption onto the walls was observed. Figure 5b shows a set of images from a second measurement where the bottom microfluidic channel contained a solution of fluorescent 20 nm polymer nanoparticles. In these measurements, single nanoparticles could be tracked traversing a nanochannel (275 nm width × 100 nm height × 200 μm length) under low applied voltages (typically +0.8 V). At this voltage, a nanoparticle velocity of 42 μm/s was observed. Occasionally, the nanoparticles got stuck in the nanochannel but could be removed by either applying higher voltages or reversing the voltage.

Nanochannel Network Fabrication. In addition to continuous parallel nanochannel arrays, a more complex LPNE fabrication process was used to create crossed nanochannel networks. The fabrication of crossed nanochannels is important for various electrophoresis applications (e.g., sample injection and separations[3] and sorting[38,39]); crossed nanochannels typically can only be generated by FIB, EBL, or IL based nanochannel fabrication techniques. In this demonstration experiment, a network of crossed nanochannels was created from a crossed nanowire master. The master was fabricated via two sequential LPNE depositions as shown schematically in Figure 6. An array of parallel nanowires with dimensions 160 nm width × 60 nm height × 2 cm length was first created by the LPNE process (steps 1a−d in Figure 1). The LPNE process was then performed a second time in a perpendicular direction (Figure 6a−c). Note in Figure 6b that sections of the original nanowire array are exposed to the second gold electrodeposition step, so that the resultant crossed nanowire array has periodic structure that includes two widths of nanowires as depicted in Figure 6c. An SEM image of a crossed nanowire master created by this process is shown in Figure 6d and verifies the structure of the crossed nanowire network. This LPNE nanowire master pattern is then copied to an h-PDMS replica, and a crossed nanochannel network is formed by O_2 plasma bonding to a glass substrate. Figure 6e,f shows 40× fluorescence images (cropped for comparison to Figure 6d and full frame, respectively) of a dye-filled network created by this process.

Note that the two different sizes of nanowires in the LPNE master result in a nanochannel network with a pattern of two different cross sectional areas (10^4 nm^2 and 1.5 × 10^5 nm^2). While there are many potential applications for these crossed nanochannel networks, we note the volume of one 60 nm × 150 nm × 10 μm segment is ∼100 aL and contains approximately 1500 dye molecules.

A distinguishing feature of the NIL method described here is its ability to pattern nanofluidic networks across large areas, spanning many square centimeters. This capability derives from the wafer-scale patterning capability of the LPNE method used to prepare the nanowire-on-glass master. To demonstrate the fabrication of nanochannels on a large area, a series of fluorescent images taken at increasing magnifications is shown in Figure 7. A rectangular section (1.3 × 3.5 mm) of a fluorescent micrograph taken at 4× magnification (Figure 7a) documents the fabrication of a network of crossed nanofluidic channels from a sample with the same dimensions as the one in Figure 6. The horizontal checkered bright regions are 250 μm wide microfluidic channels supported by a 2D lattice of 10 μm PDMS pillars, while the dark regions contain the crossed nanochannel networks. At 4× magnification using short integration times, the nanochannels are not visible; they become apparent at 10× magnification as shown in a 0.3 × 1.5 mm rectangular section in Figure 7b. The crossing nanochannels have been aligned ±45° to the microchannels. To clearly observe both sizes of nanochannels, a small region of Figure 7b is shown at 20× magnification in Figure 7c. All

dx.doi.org/10.1021/ac3007285 | Anal. Chem. 2012, 84, 5053−5058

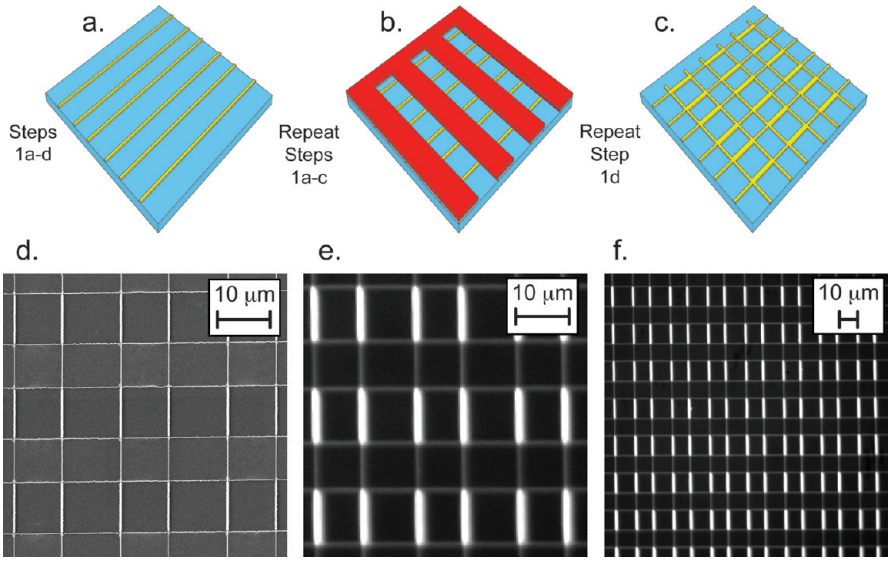

Figure 6. Crossed nanochannel network fabrication and characterization. (a–c) Schematic diagram showing the sequential LPNE processes for a crossed nanowire master. (d) SEM image of crossed nanowires network. The confined growth nanowires are ~150 nm in width whereas the unconfined growth nanowires are ~400 nm in width. (e) Fluorescent high magnification of a 6 × 6 nanochannel network and (f) 15 × 15 nanochannel network.

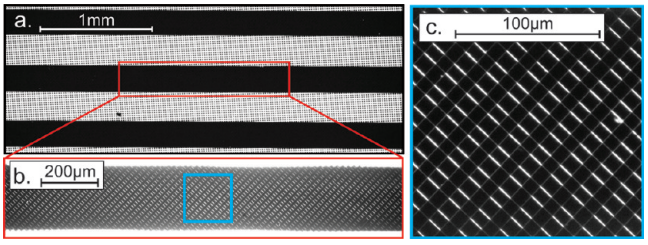

Figure 7. Large area patterning of crossed nanochannel networks imaged at increasing magnifications. Sections of (a) 4×, (b) 10×, and (c) 20× magnification fluorescent images.

images shown in this figure were taken from a sample that was 2 × 2 cm; however, larger areas can be patterned without altering the process flow shown in Figure 1.

CONCLUSION

We have developed a simple, rapid technique for fabricating macroscale, high fidelity, nanochannel arrays and networks using a master-replica process in PDMS. Instead of the use of EBL, FIB, or IL, the master is a reusable electrodeposited LPNE gold nanowire pattern that is replicated in PDMS using a thin underlayer of h-PDMS. The nanofluidic channels that are made by O_2 plasma bonding the inverse PDMS replica to a glass substrate can be easily integrated into micrometer-scale PDMS microfluidic networks and fill spontaneously with aqueous solutions. The nanofluidic channels are ionically conductive as demonstrated by the electrophoresis of fluorescent dyes and nanoparticles. These arrays have controllable dimensions and assume complex shapes, including crossed nanochannel networks. It is expected that even smaller feature sizes can be accomplished with LPNE nanowires using harder replication materials such as thermoplastics.[28,31]

AUTHOR INFORMATION

Corresponding Author

*E-mail: rmpenner@uci.edu (R.M.P.); rcorn@uci.edu (R.M.C.).

Notes

The authors declare no competing financial interest.

ACKNOWLEDGMENTS

This work is supported by grants from the National Science Foundation: CHE-1057638 (R.M.C.), CHE-0956524 (R.M.P.), and DGE-0549479 (K.C.D.).

REFERENCES

(1) Garcia, A. L.; Ista, L. K.; Petsev, D. N.; O'Brien, M. J.; Bisong, P.; Mammoli, A. A.; Brueck, S. R. J.; Lopez, G. P. *Lab Chip* **2005**, *5*, 1271.
(2) Yasui, T.; Kaji, N.; Ogawa, R.; Hashioka, S.; Tokeshi, M.; Horiike, Y.; Baba, Y. *Anal. Chem.* **2011**, *83*, 6635.
(3) Kato, M.; Inaba, M.; Tsukahara, T.; Mawatari, K.; Hibara, A.; Kitamori, T. *Anal. Chem.* **2010**, *82*, 543.
(4) Wang, Y. C.; Stevens, A. L.; Han, J. Y. *Anal. Chem.* **2005**, *77*, 4293.
(5) Chung, S.; Lee, J. H.; Moon, M. W.; Han, J.; Kamm, R. D. *Adv. Mater.* **2008**, *20*, 3011.
(6) Contento, N. M.; Branagan, S. P.; Bohn, P. W. *Lab Chip* **2011**, *11*, 3634.
(7) Guan, W. H.; Fan, R.; Reed, M. A. *Nat. Commun.* **2011**, 2.
(8) Riehn, R.; Lu, M. C.; Wang, Y. M.; Lim, S. F.; Cox, E. C.; Austin, R. H. *Proc. Natl. Acad. Sci. U.S.A.* **2005**, *102*, 10012.
(9) Lim, S. F.; Karpusenko, A.; Sakon, J. J.; Hook, J. A.; Lamar, T. A.; Riehn, R. *Biomicrofluidics* **2011**, 5.
(10) Jo, K.; Dhingra, D. M.; Odijk, T.; de Pablo, J. J.; Graham, M. D.; Runnheim, R.; Forrest, D.; Schwartz, D. C. *Proc. Natl. Acad. Sci. U.S.A.* **2007**, *104*, 2673.
(11) Reisner, W.; Larsen, N. B.; Silahtaroglu, A.; Kristensen, A.; Tommerup, N.; Tegenfeldt, J. O.; Flyvbjerg, H. *Proc. Natl. Acad. Sci. U.S.A.* **2010**, *107*, 13294.
(12) Reccius, C. H.; Mannion, J. T.; Cross, J. D.; Craighead, H. G. *Phys. Rev. Lett.* **2005**, 95.
(13) Tegenfeldt, J. O.; Prinz, C.; Cao, H.; Chou, S.; Reisner, W. W.; Riehn, R.; Wang, Y. M.; Cox, E. C.; Sturm, J. C.; Silberzan, P.; Austin, R. H. *Proc. Natl. Acad. Sci. U.S.A.* **2004**, *101*, 10979.
(14) Reisner, W.; Beech, J. P.; Larsen, N. B.; Flyvbjerg, H.; Kristensen, A.; Tegenfeldt, J. O. *Phys. Rev. Lett.* **2007**, 99.
(15) Menard, L. D.; Ramsey, J. M. *Nano Lett.* **2011**, *11*, 512.
(16) Liang, X. G.; Chou, S. Y. *Nano Lett.* **2008**, *8*, 1472.

(17) Chantiwas, R.; Park, S.; Soper, S. A.; Kim, B. C.; Takayama, S.; Sunkara, V.; Hwang, H.; Cho, Y. K. *Chem. Soc. Rev.* **2011**, *40*, 3677.
(18) Duffy, D. C.; McDonald, J. C.; Schueller, O. J. A.; Whitesides, G. M. *Anal. Chem.* **1998**, *70*, 4974.
(19) Saleh, O. A.; Sohn, L. L. *Nano Lett.* **2003**, *3*, 37.
(20) Sen, Y.-H.; Jain, T.; Aguilar, C. A.; Karnik, R. *Lab Chip* **2012**, *12*, 1094.
(21) Pagliara, S.; Chimerel, C.; Langford, R.; Aarts, D. G. A. L.; Keyser, U. F. *Lab Chip* **2011**, *11*, 3365.
(22) Angeli, E.; Manneschi, C.; Repetto, L.; Firpo, G.; Valbusa, U. *Lab Chip* **2011**, *11*, 2625.
(23) Schmid, H.; Michel, B. *Macromolecules* **2000**, *33*, 3042.
(24) Huh, D.; Mills, K. L.; Zhu, X. Y.; Burns, M. A.; Thouless, M. D.; Takayama, S. *Nat. Mater.* **2007**, *6*, 424.
(25) Mills, K. L.; Huh, D.; Takayama, S.; Thouless, M. D. *Lab Chip* **2010**, *10*, 1627.
(26) Park, S. M.; Huh, Y. S.; Craighead, H. G.; Erickson, D. *Proc. Natl. Acad. Sci. U.S.A.* **2009**, *106*, 15549.
(27) Chou, S. Y.; Krauss, P. R.; Renstrom, P. J. *Appl. Phys. Lett.* **1995**, *67*, 3114.
(28) Chou, S. Y.; Krauss, P. R.; Renstrom, P. J. *J. Vac. Sci. Technol., B* **1996**, *14*, 4129.
(29) Chou, S. Y.; Krauss, P. R.; Zhang, W.; Guo, L. J.; Zhuang, L. *J. Vac. Sci. Technol., B* **1997**, *15*, 2897.
(30) Li, M. T.; Wang, J. A.; Zhuang, L.; Chou, S. Y. *Appl. Phys. Lett.* **2000**, *76*, 673.
(31) Liang, X. G.; Morton, K. J.; Austin, R. H.; Chou, S. Y. *Nano Lett.* **2007**, *7*, 3774.
(32) Cao, H.; Yu, Z. N.; Wang, J.; Tegenfeldt, J. O.; Austin, R. H.; Chen, E.; Wu, W.; Chou, S. Y. *Appl. Phys. Lett.* **2002**, *81*, 174.
(33) Xia, Q. F.; Morton, K. J.; Austin, R. H.; Chou, S. Y. *Nano Lett.* **2008**, *8*, 3830.
(34) Xiang, C. X.; Kung, S. C.; Taggart, D. K.; Yang, F.; Thompson, M. A.; Guell, A. G.; Yang, Y. A.; Penner, R. M. *ACS Nano* **2008**, *2*, 1939.
(35) Menke, E. J.; Thompson, M. A.; Xiang, C.; Yang, L. C.; Penner, R. M. *Nat. Mater.* **2006**, *5*, 914.
(36) Xiang, C. X.; Yang, Y. G.; Penner, R. M. *Chem. Commun.* **2009**, 859.
(37) Kang, H.; Lee, J.; Park, J.; Lee, H. H. *Nanotechnology* **2006**, *17*, 197.
(38) Riehn, R.; Austin, R. H.; Sturm, J. C. *Nano Lett.* **2006**, *6*, 1973.
(39) Fu, J. P.; Schoch, R. B.; Stevens, A. L.; Tannenbaum, S. R.; Han, J. Y. *Nat. Nanotechnol.* **2007**, *2*, 121.